33RD CONGRESS
OF THE INTERNATIONAL COUNCIL
OF THE AERONAUTICAL SCIENCES
STOCKHOLM, SWEDEN, 4-9 SEPTEMBER, 2022

ICAS 2022 SWEDEN

APPLICATION OF THE VIRTUAL CRACK CLOSURE TECHNIQUE FOR CRACKS IN BUILT-UP PANELS

Willy Roger de Paula Mendonça, Marcelo Ricardo Bertoni Rodrigues

Embraer, Sao Jose dos Campos, Brazil

Abstract

The objective of this paper is to show the application of Virtual Crack Closure Technique (VCCT) for analysis of typical fuselage and wing built-up panels, evidencing the contribution of different load components on crack opening. In particular, this study shows through analysis, and validation with experiments, the influence on the crack of the local bending induced by the failure of a structural reinforcement element. The local bending is even more relevant for thick panels, and this aspect will be addressed in this paper. The use of robust methodologies in structural analysis contributes for the improvement of aircraft structural integrity.

Keywords: vcct, wing, nastran, propagation, crack

1. Introduction

The damage tolerance requirements for aircraft structures have leaded to extensive researches on fatigue crack propagation over the years. In order to show compliance to these requirements, usually it is necessary to determine the period of time while a structure component is able to withstand a crack growing from an initial flaw size (assuming an existing flaw), up to a critical size, which is based on the evaluation of the structure residual strength in a presence of the damage Figure 1 schematically illustrates the size of the crack as a function of the number of flights. Based on these data, an inspection plan must be established to guarantee the detection of the crack before it reaches the critical size.

Crack growth analysis provides a quantitative information related to a dynamic (fatigue) loading condition, while the residual strength analysis gives a qualitative information related to a static (critical) loading condition. Both analyses require the application of fracture mechanics concepts.

Based on a stablished failure scenario, an important and time-consuming phase of a damage tolerance analysis (DTA) consists in determinate the stress intensity factors (SIF or K) at the tip of a crack assumed to exist in the structure, for different lengths throughout a path.

A typical wing built-up panel is illustrated in Figure 2, consisting of a skin, stringers, ribs and spar. A common failure scenario requires to account for the failure of a stringer or spar (Primary component) in the crack propagation in skin (Secondary component), and residual strength of the structure.

The effects of the failure of primary component can be computed by means of geometry correction factors, also known as beta factors (β), or by taking failure into account on the reference stresses. This requires either refined finite model analyses (FEA), or previously developed factors from in-house database or from literature.

The structural engineer has extensive information and computational commercial tools (e.g. Nastran, NASGRO® [15]) available to develop a DTA. Although all these tools have proved their robustness for certified products over the years, there have been mapped some improvements and specific necessities to be implemented on an in-house tool, named DTA-Tool.

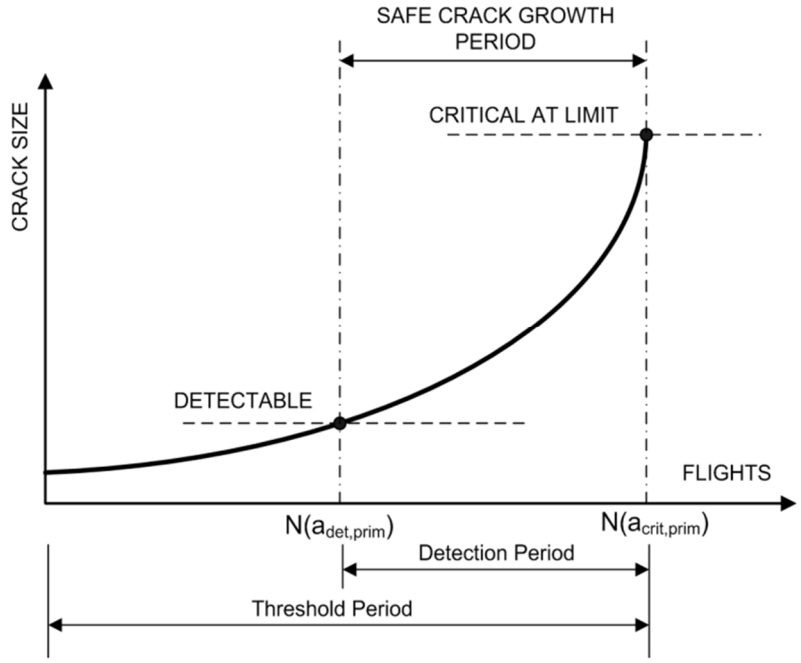

Figure 1 – Schematic diagram for definition of inspection intervals

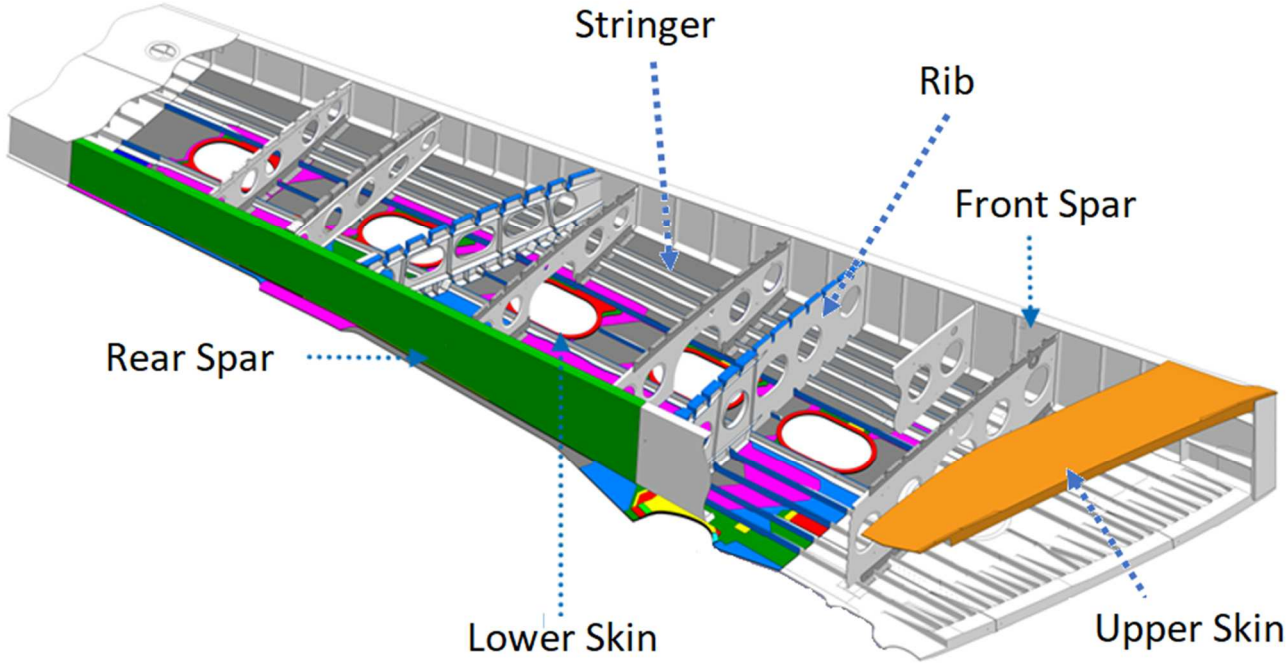

Figure 2 – Wing structure cutaway

A parametric modeling strategy was conceived for application of the VCCT methodology, through post-processing finite element analysis (FEA) results. In this work, it was introduced the local bending effects (Figure 3c) into the crack propagation analysis, which arises from the full failure of a panel stiffener.

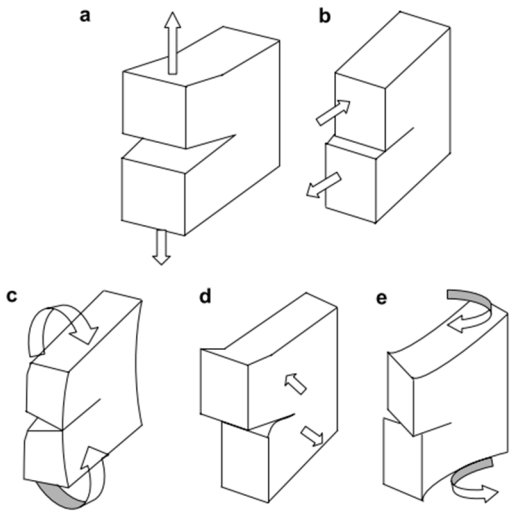

Figure 3 – Fracture modes for cracked plate under in-plane and out-of-plane loads: (a) tensile (mode-I), (b) In-plane shear (mode-II), (c) bending (mode-I), (d) out-of-plane shear (mode-II) and (e) twisting (mode-III), [7]

2. Literature Review

Crack growth analysis has become increasingly important in engineering problems in recent years. The most direct method for numerically studying crack behavior is to use fracture mechanics in conjunction with the finite element method.

Linear Elastic Fracture Mechanics (LEFM) is a sophisticated yet highly simplified theory that deals with sharp cracks in elastic bodies. As long as certain conditions are met, LEFM can be applied to any material. These conditions are predicated on the presence of all of the basic ideal conditions studied in LEFM, in which all materials are elastic except for a vanishingly small region (a point) at the crack tip. In fact, the stress near the crack tip is so high that some kind of inelasticity must occur in the crack tip's immediate vicinity.

However, if the inelastic zone is small in comparison to the body's linear dimensions (including the length of the crack), the disturbance introduced by this small inelastic region is also small. As a result, LEFM and point of failure can be correctly verified.

To study a variety of fracture problems, LEFM has been developed and implemented within commercial finite element codes. Based on the displacement field obtained from FEA, for example, SIF or strain energy release rate can be calculated. The requirement of a small process zone ahead of the crack tip is critical to the success of LEFM approaches [16].

A bibliographic review was conducted to assess the methodologies used in the calculation of the SIF, which quantifies the contribution of flexion in mode I. The primary objective was to choose a method that would be implemented in the DTA-Tool software. A numerical method was preferred because analytical methods typically have solutions constrained by geometric limits. A numerical method would be easier to implement and would make use of the results generated by the DTA-Tool software's analysis.

Most of the evaluated analytical methods dates to the 70's and 80's, including some methods already implemented in NASGRO® software, and deal with simplified problems of unreinforced plates. By not comprehending the discontinuity generated by the failed reinforcer, these methods do not provide a gain in relation to the methodology currently used. For example, the NASGRO® case TC03 employs the formulation of Roberts and Erdogan [8] to account for the effects of a remotely applied bending, and the geometry factor is simplified by the equation F2 = F1/2.

Currently, another widely applied method is the energy release method, which applies the total variation of strain energy (dU) of a FE model per a given crack length advance (dU/da), to calculate stress intensity factors, based on LEFM theory. Several works continue to be developed in this direction Melo [17] presented a work where simultaneous cracks in cooperative lugs were evaluated, the work used the energy method with the support of finite element analysis. Shaopu and Wendong [18] conducted tests and validated the results obtained by finite element models to investigate the

propagation of cracks influenced by mixed-modes (I and II). The numerical and experimental development of this work was similar to that proposed in this study.

There are methodologies that have proven to be very robust in crack propagation analysis in problems involving many physical phenomena that necessitate high fidelity models, but the computational cost required does not meet the needs of this present development. The work presented by Zaplana et al [19] makes use of high-fidelity models to investigate cracks in cold-worked holes; in the numerical development, they used XFEM to apply the J-integral methodology.

Works evaluated on the literature review on the VCCT showed that this method can capture adequately the influence of bending, by computing strain energy release rate (dU/da) from the crack tip rotations and moments.

Past literature studies are most over simplified cases of plates [7][11]. Others studies apply FE solid models to address the contact between the crack surfaces [2][3][4], which is influenced by the loading (bending) and thickness of the structure and, even in this case, experimental validations are lacking.

One of the few experimental tests was developed in the work of Corbani [1], to validate a new proposal of analytical solution, still applicable to simplified geometries and boundary conditions.

Although it is a relevant phenomenon, contact was not the object of this study, due to the following reasons:

- it affects mainly corner crack propagation phases, which is currently carried out via NASGRO®.
- Its representation is not compatible to parametric models based on plate/shell elements.
- lack of experiments results.

The use of VCCT in delamination analysis in composite structures is widely used; the study by Jokine, Kanerva, and Saarela [6] exemplifies this well.

Following a thorough bibliographic review, it was determined that the VCCT could be used to capture the effects of out-of-plane bending on crack propagation. Another observation is that no developments that evaluated the phenomenon investigated in aeronautical structures as proposed in this development were discovered.

3. Methodology

The main objective of this development was to improve the predictability of growth rate of relatively small cracks, in the phase where local bending induced by failure of a stiffener has more influence on the results

DTA-Tool is a pre- and post-processing software that generates parametric finite element models, and post-processes the analysis forces and displacement results. The models are designed to simulate the crack advances by multiple steps of mesh opening, with a local refined mesh for an accurate calculation of stress intensity factor (K), by means of the VCCT technique, as detailed in along this section. The combination of the secondary bending effects to the axial loading effects is done by the superposition principle, presented in section 3.4.

The analysis process for built-up panels is illustrated by a flowchart in section 3.5, which shows the integration of ih-house DTA-Tool with commercial software.

The results of the experimental tests presented in Section 4 are employed for correlation to analysis results, which are therefore considered validated, according to Section 5.

3.1 Built-up panel finite element model

Parametric FEM employs shell-type elements (NASTRAN PSHELL/CQUAD4) to represent panel skin and stiffeners, and spring-type elements (NASTRAN CBUSH and CFAST) to represent the fasteners joining the parts.

Crack advance is simulated through mesh separation technique, in which a pair of coincident skin nodes are joined together or are unzipped, depending on the set of Multi-Point Constraints (MPC) equations. Thus, each crack step requires a different FEA, each one performed with the same basic model, but with a different MPC combination. Figure 4 shows the simulation of crack growth.

Uniform remote stress is applied at panel forward and rear edges. Constraints conditions are defined

specifically for each damage scenario, aimed to a correct account of global and local bending, and depend on which stiffener component is failed and on the crack position.

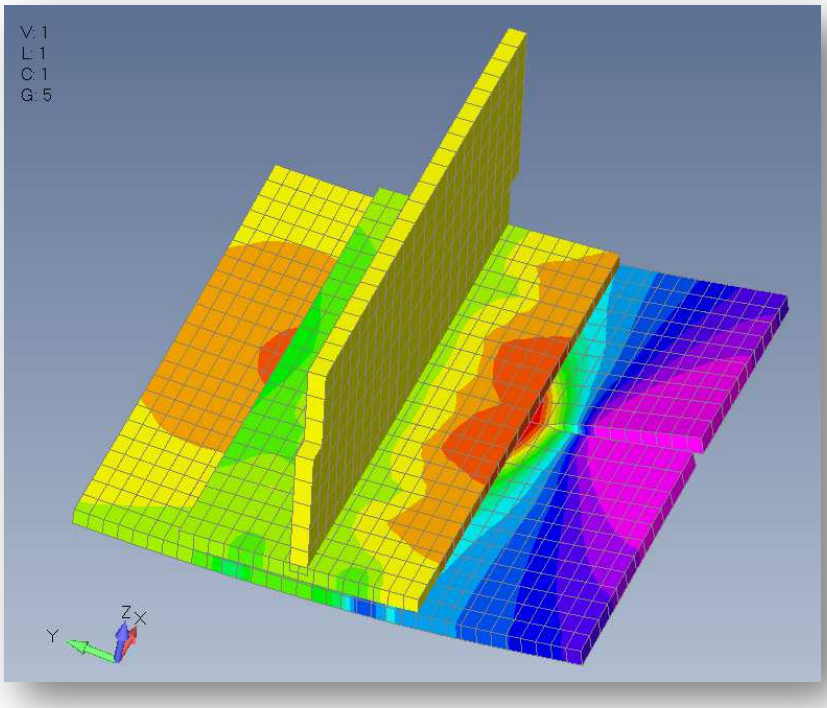

Figure 4 – Crack growth simulation in FEA

All materials are defined as linear elastic in FE model, whose analysis results can be employed for determination of stress intensity factor by the VCCT technique, as long as the plastic zone size is within the limits of application of the LEFM.

3.2 Stress intensity factor

The concept of stress intensity factor (K) is a result of the bi-dimensional analysis of the stress field at the crack tip. This analysis was carried out by Williams in 1957 [12], considering Westergaard's work, [13]. Using a coordinates system centered in the crack tip and according to William's analysis, the near crack tip components of the stress field are proportional to $K/r^{1/2}$, where K is the stress intensity factor. The crack opening may correspond to one of the three basic cases, the opening mode, the sliding mode and the tearing mode, or to any of their combination; thus, there are three basic stress intensity factor values denoted with the subscripts I, II and III. For each mode, the stress field in the crack tip region may be calculated using the expressions:

$$\lim_{r\to 0} \sigma_{ij}^{(I)} = \frac{K_I}{\sqrt{2\pi r}} f_{ij}^{(I)}(\theta) \tag{1}$$

$$\lim_{r\to 0} \sigma_{ij}^{(II)} = \frac{K_{II}}{\sqrt{2\pi r}} f_{ij}^{(II)}(\theta) \tag{2}$$

$$\lim_{r\to 0} \sigma_{ij}^{(III)} = \frac{K_{III}}{\sqrt{2\pi r}} f_{ij}^{(III)}(\theta) \tag{3}$$

where r and θ are the polar coordinates in the system of axes having the origin at the crack tip. According to Williams' analysis, the components of the stress field can be written as series expansions; from this expansion, the stress intensity factors can be calculated from the stress field in the crack tip.

3.3 Virtual crack closure technique

This technique was proposed by Rybicki and Kanninen in 1977, [10]. A review of VCCT can be is found in the report referred in [5].

The VCCT criterion uses the principles of LEFM and, therefore, is appropriate for problems which brittle crack propagation occurs along predefined surfaces. VCCT assumes that the strain energy released when a crack is extended by a certain amount is the same as the energy required to close the crack by the same amount.

Figure 4 illustrates a case in pure Mode I loading. Then, assuming that the crack closure is governed by linear elastic behavior, the energy to close the crack and, consequently, the energy to open the crack, is calculated by equation (4).

$$-\frac{1}{2}\frac{F_{v,2,5}v_{1,6}}{\Delta A} = G_I, \quad \Delta A = \delta u b \tag{4}$$

where $F_{v,2,5}$, $v_{1,6}$, δu, b and G_I denote node reaction force at the nodes 2 and 5, displacement between released nodes 1 and 6, crack extension as the length of the element at the crack front, the width and energy release rate respectively.

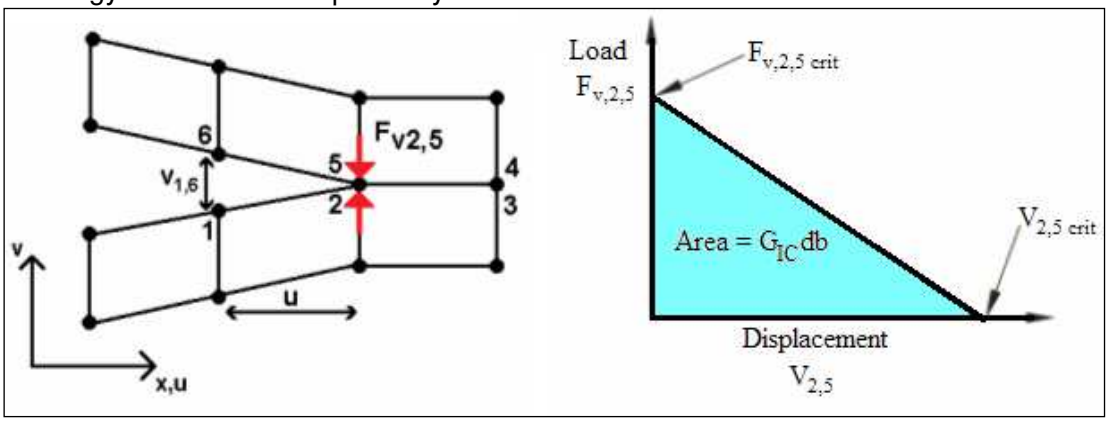

Figure 4 – Vcct crack growth criterion

Similar arguments and equations can be written in two dimensions for Mode II and for three-dimensional crack surfaces including Mode III.

3.4 Superposition principle

Whereas compounding technique consists in multiplication of geometry factors, aimed to taking into account combination of different geometries, superposition principle consists in addition of stress intensity factors due to different loading conditions, under the same crack opening mode. For example (Figure 5), in a combination of beading and tension loads, the total crack tip stress, from the equations that describes the stress field at crack tip [14], is:

$$\sigma_{ij} = \frac{K_{ben}}{\sqrt{2\pi r}} f_{ij}(\theta) + \frac{K_{ten}}{\sqrt{2\pi r}} f_{ij}(\theta) \tag{5}$$

The total stress intensity is:

$$K_{tot} = K_{ten} + K_{ben} \tag{6}$$

It should be emphasized that superposition of stress intensities of different modes of loading is not possible [14].

After the superposition is complete, β must be obtained by selecting a suitable reference stress. Generally, all damage tolerance analysis is based on $K = \beta\sigma\sqrt{\pi a}$. Assume a combined bending and tension case are as show. The stress intensity is:

$$K_{tot} = \beta_{ben}\sigma_{ben}\sqrt{\pi a} + \beta_{ten}\sigma_{ten}\sqrt{\pi a} \tag{7}$$

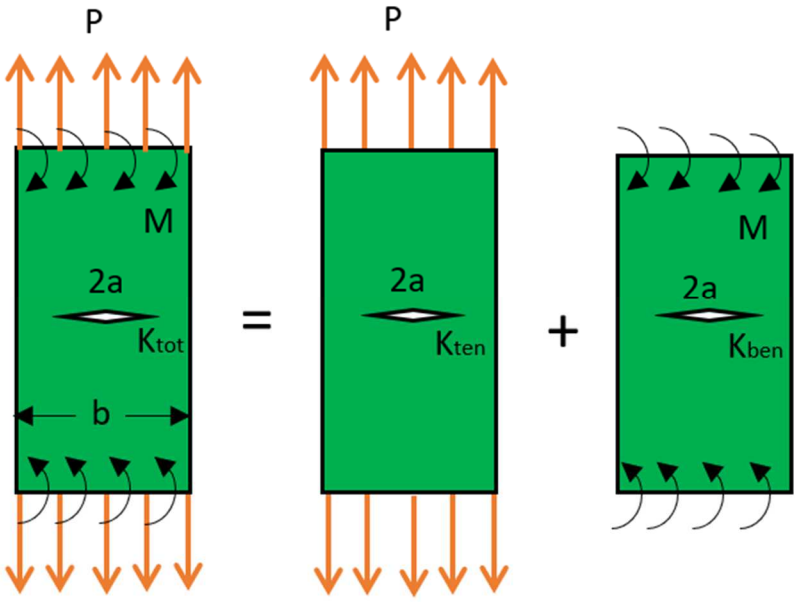

Figure 5 – Example of superposition principle in (K) calculation

To obtain β for the combination a reference stress must be selected. This can be any σ_{ben}, σ_{ten}, $\sigma_{tot} = \sigma_{ben} + \sigma_{ten}$, or any other suitable stress. Selection σ_{ten} leads to:

$$K = (\beta_{ben}\frac{\sigma_{ben}}{\sigma_{ten}} + \beta_{ten})\sigma_{ten}\sqrt{\pi a} = \beta\sigma_{ten}\sqrt{\pi a} \quad (8)$$

$$\beta = \beta_{ten} + \beta_{ben}.\frac{\sigma_{ben}}{\sigma_{ten}} \quad (9)$$

3.5 Analysis of the Built-up Panel

The main results obtained with DTA-Tool are: geometric correction factors (β) and stress intensity factor curves (K). The crack propagation analysis was performed in NASGRO®, applying the β calculated by the DTA-tool, in combination to β from a NASGRO® library that takes into account fastener hole effects (compound method).

In fact, NASGRO® has libraries or solutions for geometry factors for different crack scenarios - geometry and loading conditions, however most for one single part problem. Therefore, the influence of one part on other is usually determined by in-house solutions or complementary FE analysis. Figure 6 shows the schematic analysis process, which evolves basically three computational tools: a FEA solver, such as NASTRA, DTA-tool for pre- and post-processing and calculation of beta factors, and NASGRO for crack propagation analysis, different crack case (TC03, TC13, TC19, TC23) can be selected for compound with K from DTA-Tool (see figure 6a).

Regarding FEA (see figure 6b), linear static analysis (SOL 101) or non-linear geometric analysis (SOL 106) may be applied, depending on specifics characteristics of each problem.

The VCCT equations inserted in the DTA-Tool calculate the work (W) performed at the crack opening and then the stress intensity factor (K) and finally the geometric correction factor (β). The analysis is carried out separately for the bending and normal forces in mode-I, according to the formulation presented below. Finally, the factors are combined using the tension stress as a reference, see section 2.3.

$$W_i = \frac{1}{2.t.\Delta a}.\left(F_i^{close}\left(u_i^{node\_f1} - u_i^{node\_f2}\right)\right), i = 1, \dots, 6 \quad (10)$$

$$K_{axial} = \sqrt{W_{axial}.E} \quad (11)$$

$$K_{bend} = \sqrt{W_{bend}.E} \quad (12)$$

$$\beta_{ten} = \frac{K_{ten}}{\sigma_{ten}.\sqrt{\pi.a}} \tag{13}$$

$$\beta_{ben} = \frac{K_{ben}}{\sigma_{bend}\sqrt{\pi.a}} \tag{14}$$

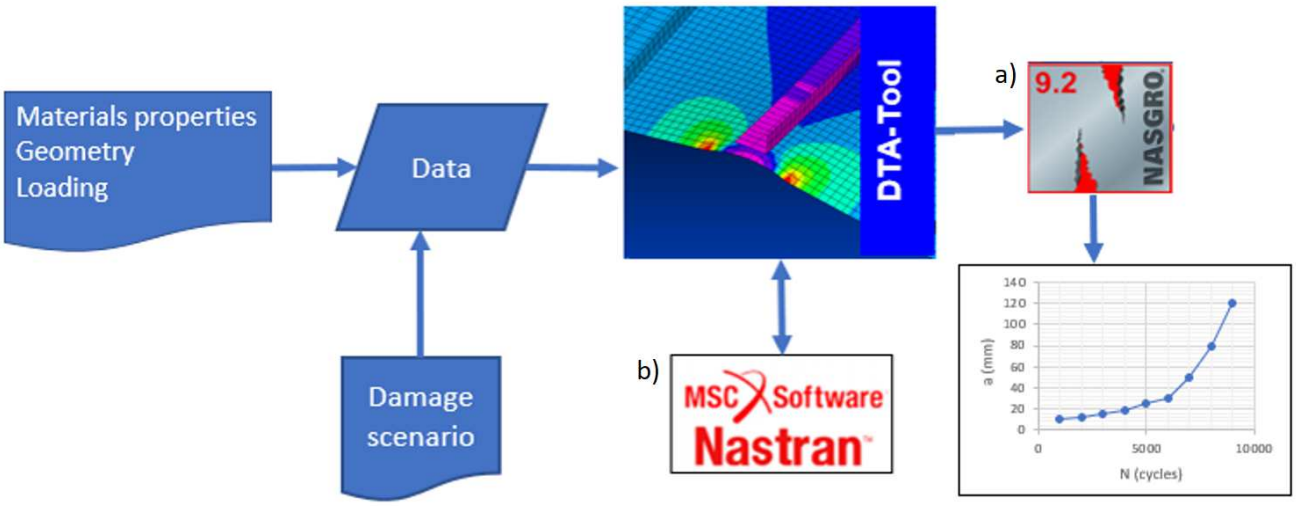

Figure 6 – Schematic analysis process

4. Experiments

The experimental results of two different configurations of wing built-up panels were employed for validation of analysis methodology. The selection of this experiments was motivated by the thickness ranges, and consequent presence of significant local bending effects. Figure 7 show the specimens subjected to crack propagation tests under cyclic loads.

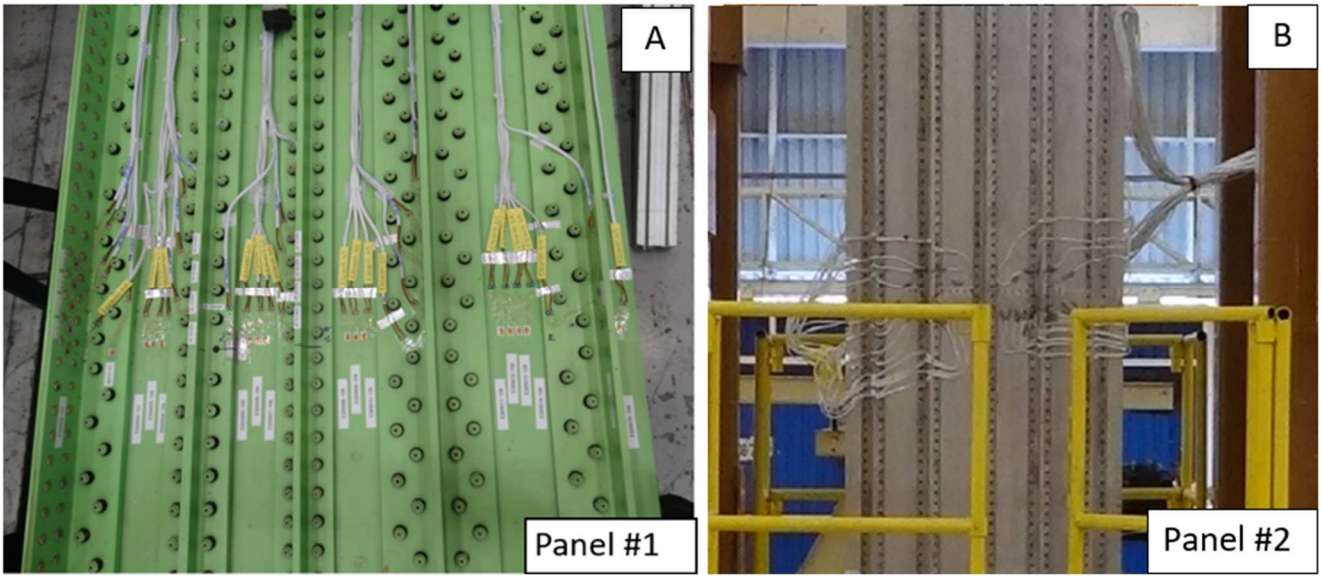

Figure 7 – Representative wing built-up panels

Boundary conditions and test loads: Constant amplitude cyclic loading is applied, with level representative of typical aircraft flights. Loading was applied by hydraulic actuators at the ends of the panels. Because of the geometric asymmetry of the cross-section (different stringers along width) in panel 1, researchers chose a system with a constant displacement at the end (see figure 8a), whereas for panel 2, where the cross section is symmetrical (all stringers are identical), researchers used a system with a constant stress (see figure 8b).

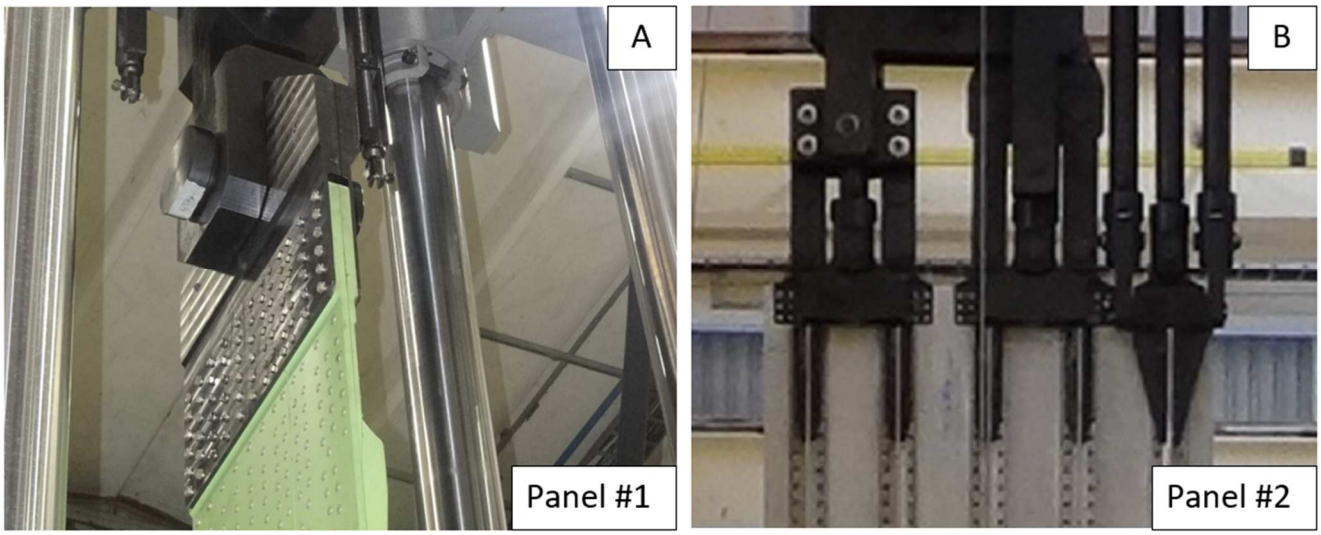

Figure 8 – Representative wing built-up panels

The panels' boundary conditions also received an anti-bending system to prevent displacement out of the plane in locations where there were Ribs; figure 9 illustrates the system used in panel 1.

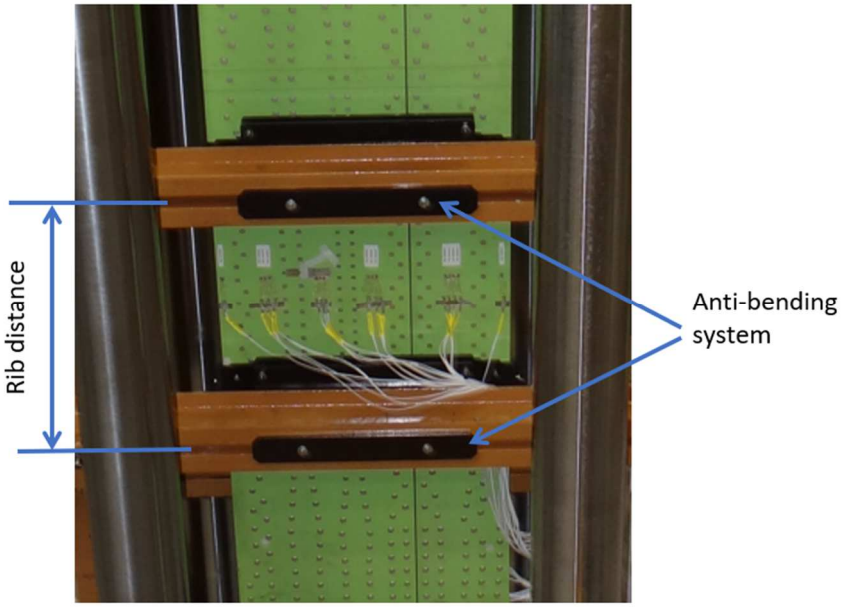

Figure 9 – Anti-bending system

5. Results and Discussion

In this section, correlations between analysis and experimental results are presented for the two built-up panel configurations, regarding crack propagation *vs.* load cycle curves. First, FE model representativeness is proven through the correlation of strains measured experimentally and the ones obtained by finite element analysis (FEA).

5.1 Correlations for Panel 1

The results presented here refer to the crack propagation resulting from the artificial damage inserted in the panel illustrated in Figure 10. The damage comprises the total failure of the stringer (primary element) and a through crack of 23.4 mm in skin (secondary element).

The stringer failure in the panel was chosen because it causes local bending, which influences the development of the short crack by generating an additional mode-I opening effort. The study's goal was to show that incorporating this local effort in the calculation of K is relevant in predicting the propagation of short cracks and that it should only be considered after the crack becomes a through

crack in the thickness.

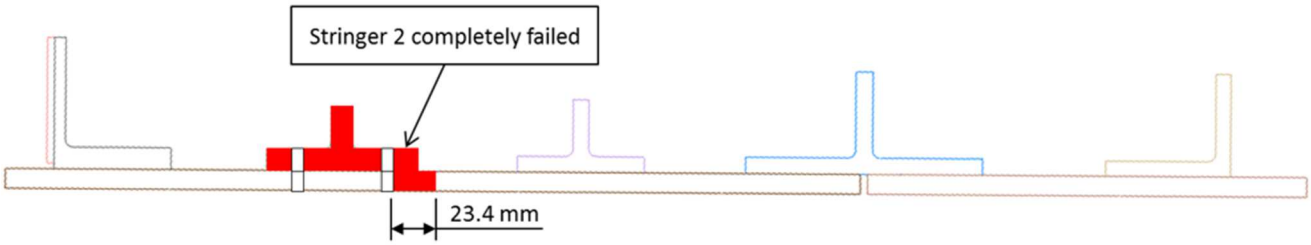

Figure 10 – Artificial damage (Schematic)

Before simulating propagation, the first step is to perform static correlation. This is required to ensure that the FEM accurately represents the panel that was tested. As previously stated, the installed gages (see figure 11a) are intended to monitor the panel's region of greatest interest, attempting to verify the loading flow in the panel. The primary goal was to measure local bending.

To have a greater representation in the correlation in the failed section, the holes of the fasteners were represented (see figure 11b). These fasteners were excluded from the model because they lost effectiveness with the existence of the damage, that is, they do not transmit load, i.e., they no longer transmit load.

Figure 12 depicts a typical graph for correlating simulated static results with experimental ones. The abscissa represents strain measurements obtained during testing, and the ordinate represents strain obtained during simulation; the results are always compared for the same direction and loading effort.

The points shown are the result of a pair of strain results (experimental and simulation); if the point is on the dashed line that is inclined at 45° in the quadrant, users conclude that the correlation was perfect. In practice, this is extremely difficult to achieve for all the verified points because the panel, rig, and loading system are not perfect, being subjected to a variety of disturbances that influence the measurement, such as manufacturing tolerance, strain gauge positioning, friction, clearances, loading variations, and so on.

So, based on the specific practice of each development, researchers can adopt correlation tolerances to evaluate it. Typically, the dataset is evaluated as a whole, with a bad correlation point being evaluated only if it deviates significantly from the specified tolerances. The correlation obtained in figure 12 was deemed adequate for development.

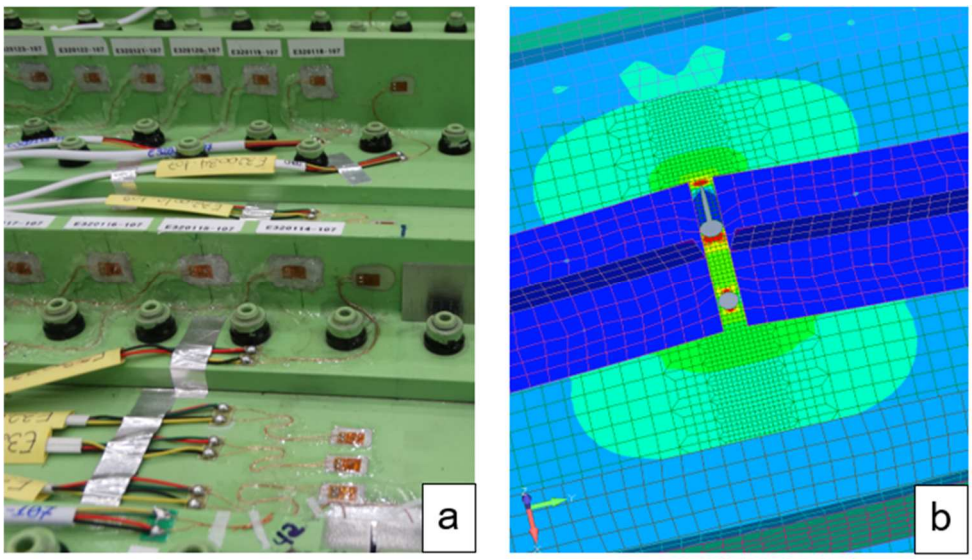

Figure 11 – Strain gauges installed in panel (a) and stress field at failure region (b)

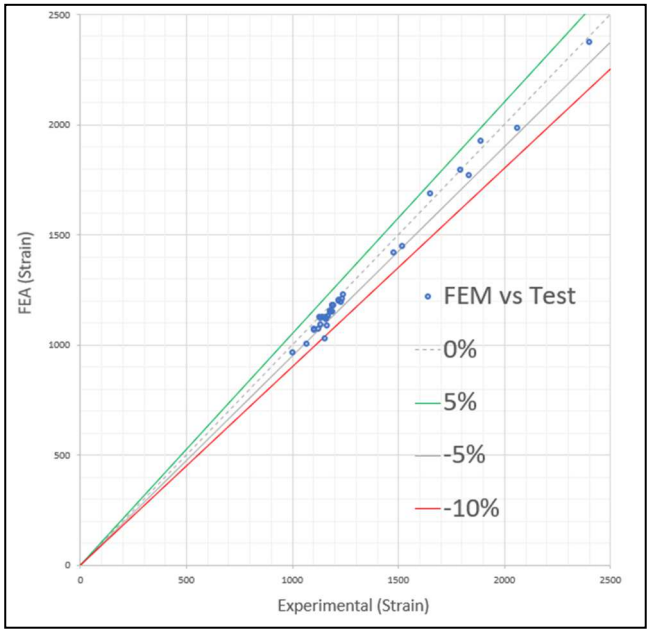

Figure 12 – Static correlation for Panel 1

Figure 13 presents the propagation of a crack tip in the structural element in which it is located, in this case the skin crack. Find the number of loading cycles (N) in the abscissa and the length (a) between the crack tip and its origin in the ordinates; notice that for N=0, a=23.4, which corresponds to the artificial damage introduced in the panel (see, figure 10).The propagation results from the test (red circles); crack propagation using the β calculated by the energy method (pink line); crack propagation calculated with the β_{ten} using only the contribution of membrane stress (black line); and crack propagation with $\beta_{ten+ben}$ calculated using bending and membrane contributions obtained by VCCT.

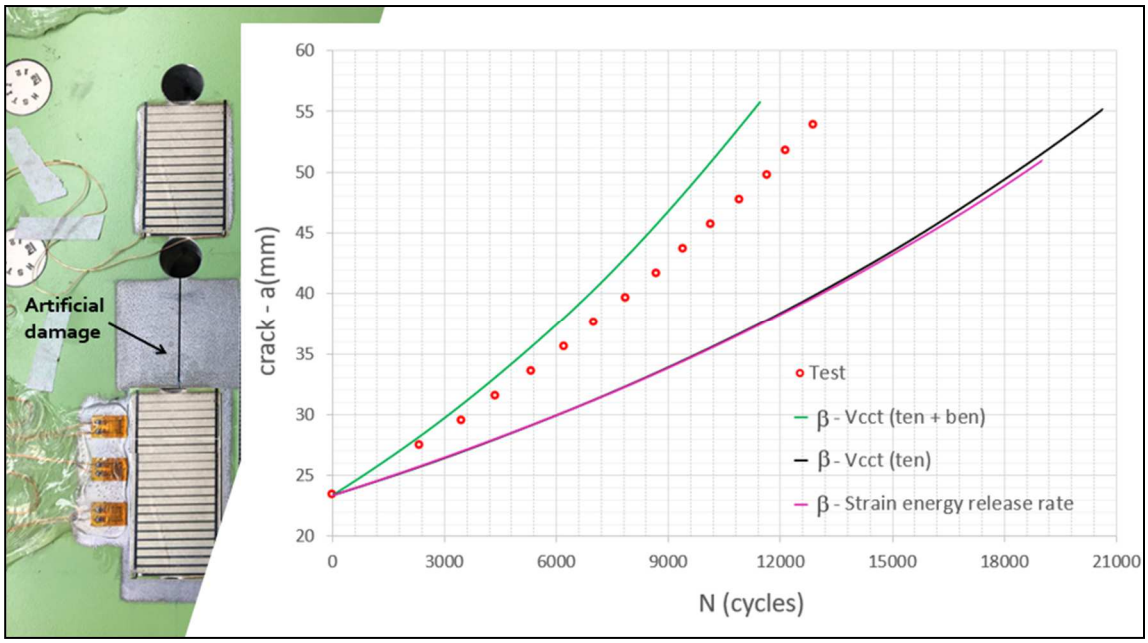

Figure 13 – Crack propagation correlation – Panel 1

From this result, the first observation is that the energy method and VCCT considering only the membrane effort (tension) are equivalent, as already verified in other studies, but they are not conservative in this propagation phase, also requested by a local bending. The second statement is that when including bending stress in the VCCT analysis results in a conservative propagation curve, which correlates better.

This method performs the calculation of beta in the medium fiber, the propagation obtained from the test was measured in the external fiber, however according to the results presented in the studies [1][9] there is a lag between the crack fronts on the two faces of the skin related by the proportion (bending/tension), see figure 14.

Although the bending is not constant in the evolution of the crack, a certain lag is expected. Thus, conclude that because the propagation measurement was made in the less tensioned fiber, the propagation in the average fiber of the skin tested is faster than that shown in Figure 11, which would improve the correlation and consequently reduce conservatism.

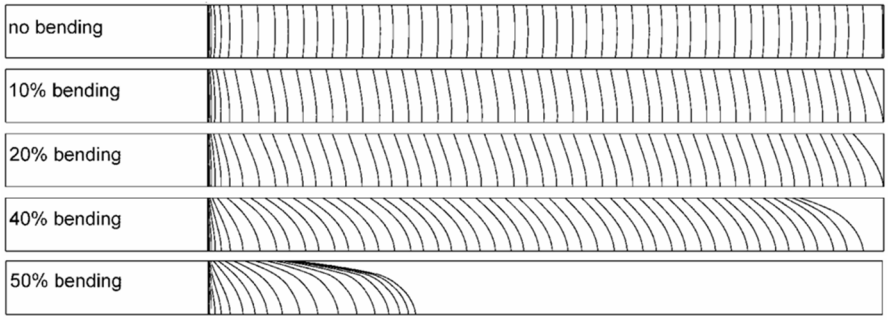

Figure 14 – Schematic drawing illustrating crack propagation as a function of bending effort [9]

The crack propagation test was beyond the 55 mm shown in figure 11, here in this study only was evaluated the short crack where the effect of local bending has greater influence.

5.2 Correlations for Panel 2

A similar study was carried out with the second panel. The primary distinction between the panels is their thickness and loading. The reference thickness in this panel is half of that used in the first panel. Figure 15 demonstrates the inserted artificial damage in panel 2. Because it is a development test that covers other development analyses, a symmetrical damage was generated in this test to provide symmetry while meeting the boundary conditions of other analyses. The initial crack propagation (shorter crack) results, on the other hand, served the purpose of this study, which was to analyze the influence of local bending in the failure region.

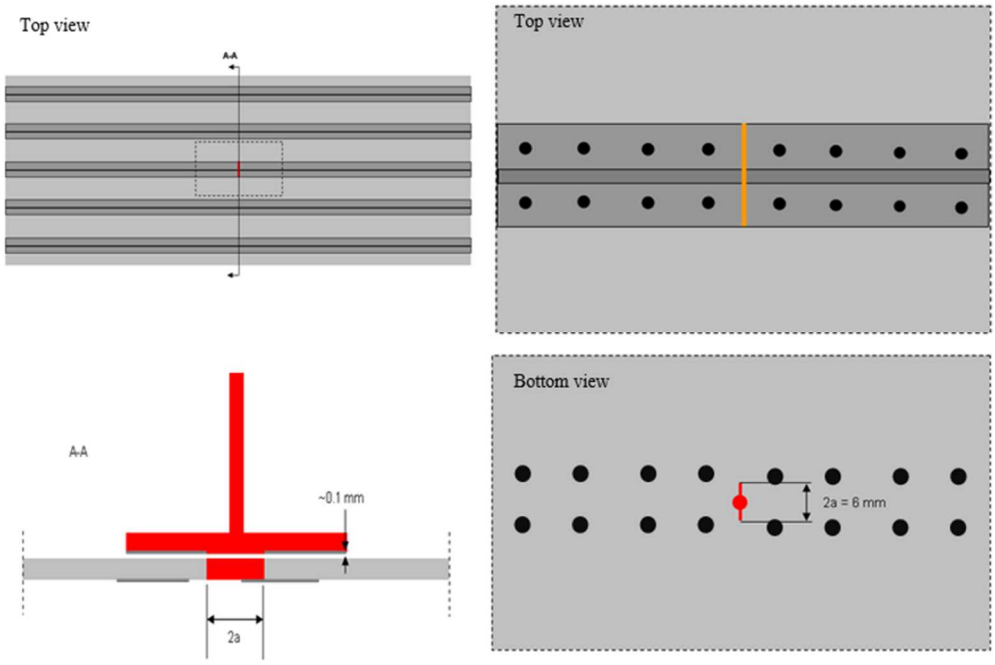

Figure 15 – Artificial damage in Panel 2 (Schematic)

Figure 16 illustrates some crack propagation simulation steppes from A to D, where static

correlations were performed with different crack sizes using acquisitions made during test execution. The aim of these correlations was to see if the model's representation was still adequate.

The static correlation shown in Figure 17 was obtained for the crack 2a = 118 mm, and the correlation points referring to stringers were obtained for the stringer adjacent to the failed stringer, in order to verify the carryover redistribution between the skin and stringer components. Panel 2's correlation was satisfactory for different crack sizes, as shown in panel 1.

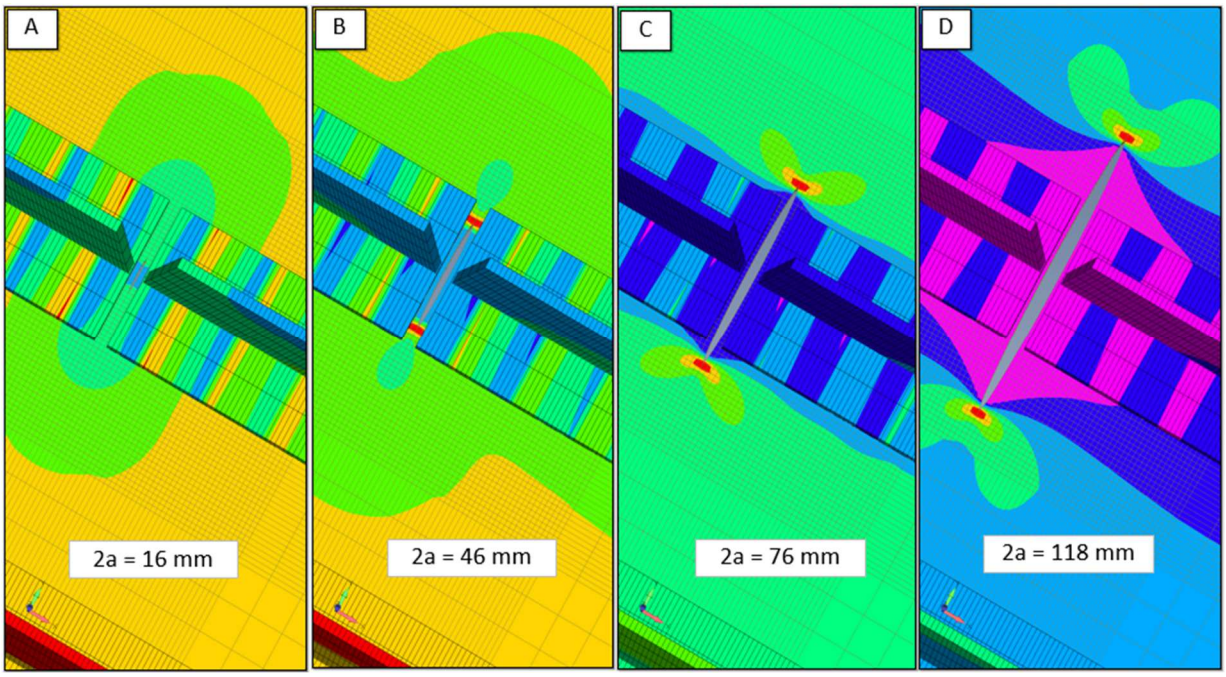

Figure 16 – FEA development for Panel 2 (a) and strain gauge correlation (b)

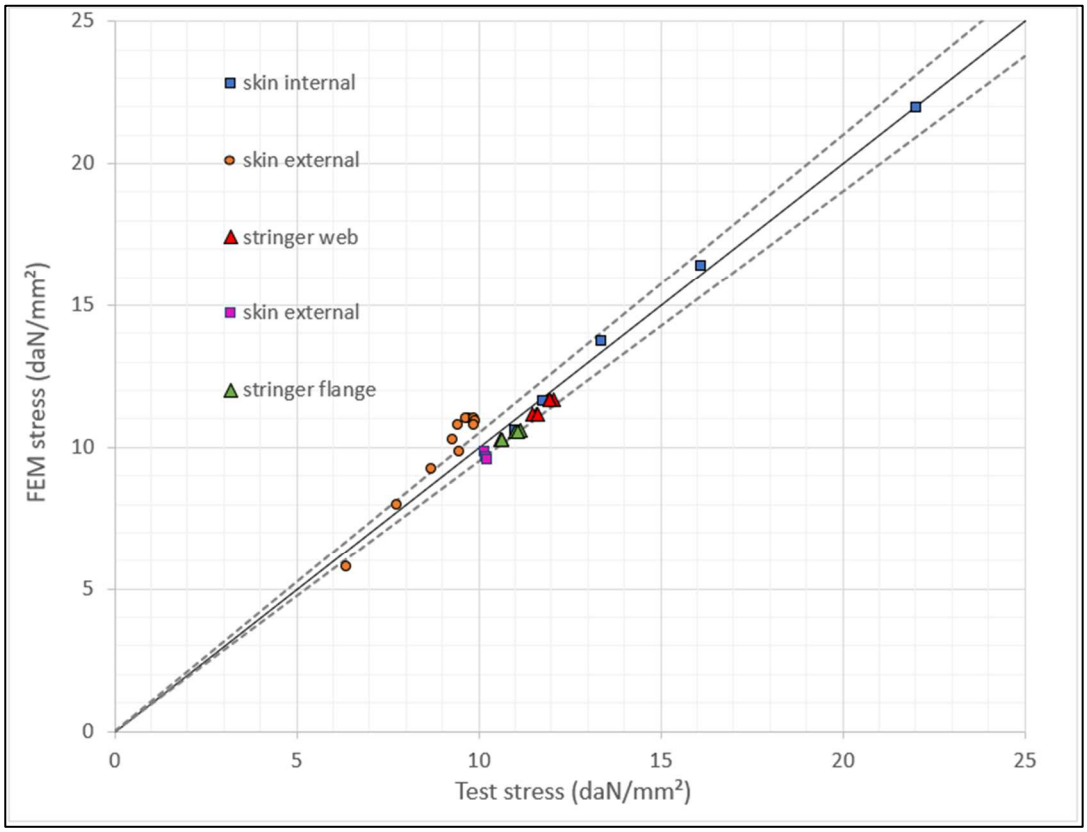

Figure 17 – FEA development for Panel 2 (a) and strain gauge correlation (b)

Figure 18 shows the crack length in the test; the figure was taken as part of the test inspection plan.

Cycle intervals are typically specified for inspectors to measure crack length and acquire strain gauges; the crack size must be determined using nondestructive testing inspection (NDI) (e.g. liquid penetrant, edge current, etc.). Other techniques, such as the crack gauge used in panel 1 (see figure 8), or digital image correlation (DIC), can be used. The crack length measurements obtained were used to generate the points shown in Figure 19's propagation correlation graph.

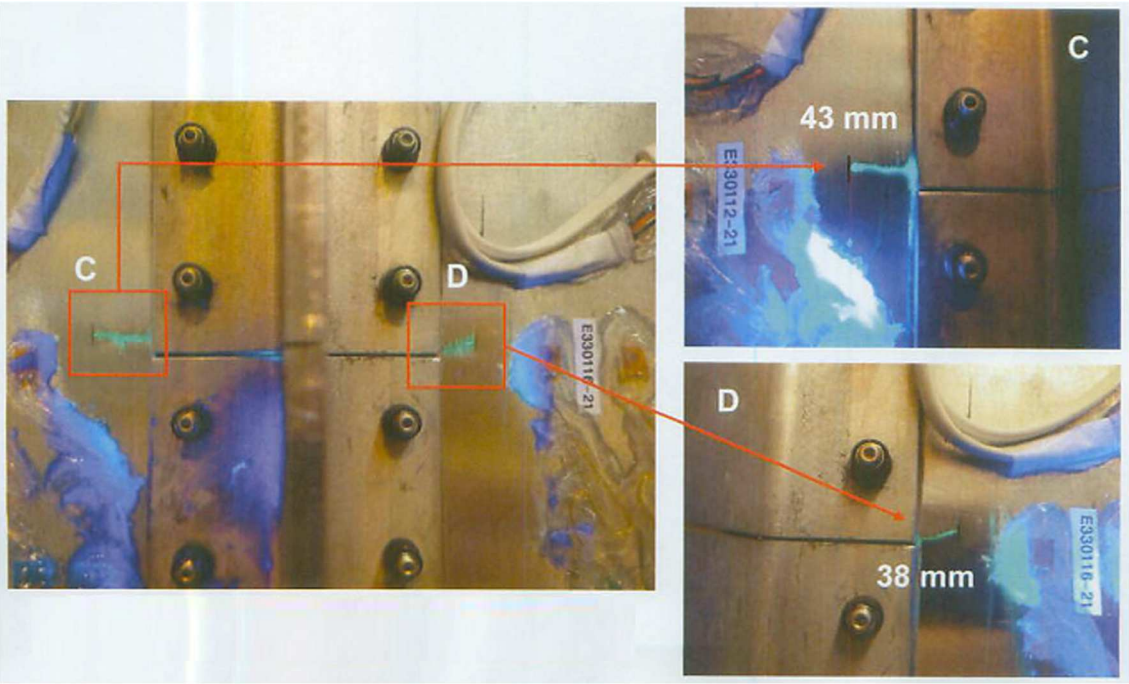

Figure 18 – Crack length

The experimental results are represented by red circles in Figure 19, and two simulated curves using the VCCT methodology with tension and bending efforts (green curve) and only with the tension effort are shown (black curve). Again, when only the tension effort was considered, the simulated result was non-conservative, whereas using both efforts produced a satisfactory fit.
Throughout the propagation curve, the simulation of this panel did not behave conservatively, among the potential hypotheses are:

- Panel 2 has less thick structural elements than panel 1, and the thickness has a strong influence on the local bending caused by the failure.
- Crack growth asymmetry. The average length between the two crack tips for the same cycles was used to generate the experimental curve shown in Figure 19. Cracks have a tendency to seek balance in their growth, but experience has shown that this is not a linear process and that it has a strong relationship with the design and materials involved. A symmetrical growth between the two crack tips was implemented in this simulation, but asymmetry can be simulated as well.
- Initial crack size measurement errors. Only one face of the panel was inspected at the start of propagation, while the crack was under the stringer cap. Asymmetry in the length of the two crack tips is possible, as are lags between the skin faces, which increases the possibility of measurement error at this stage.
- Material properties. There is some variation in the supply lot material. Specific mechanical characterizations are performed for the batch used in the production of the specimen in some developments. Supplier properties were used for this simulation.

Even though the correlation was not conservative at the start of the propagation, the simulation proved to be much more representative of the physical behavior, emphasizing the gain obtained in the prediction analyses for short cracks.

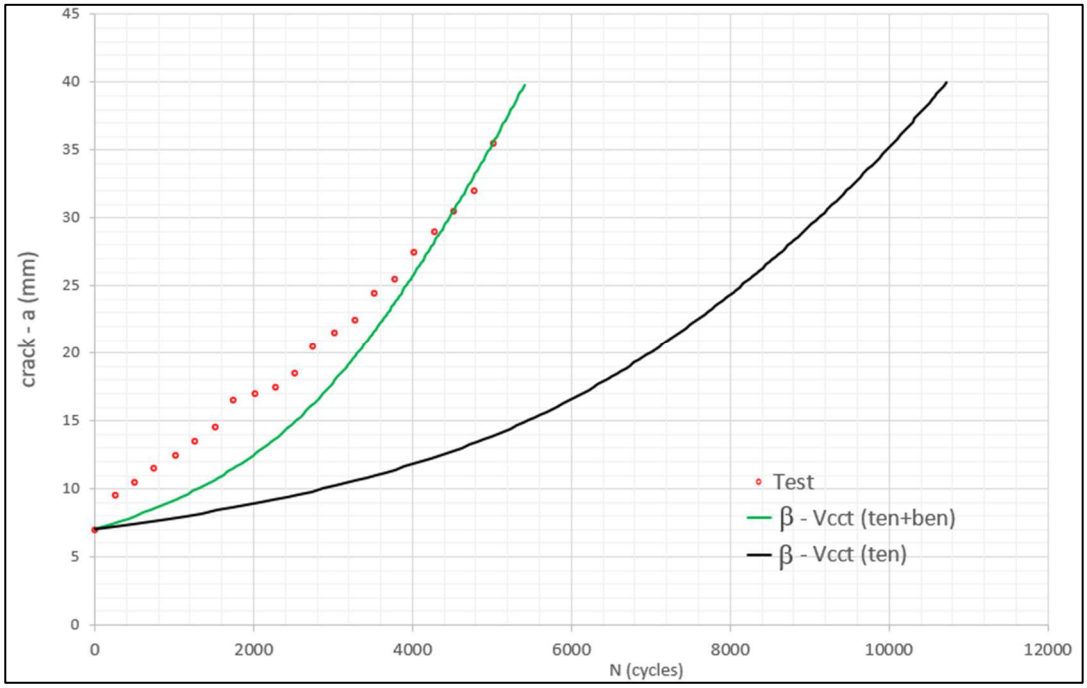

Figure 19 – Crack propagation correlation – Panel 2

6. Conclusions

The goal of this research was to show that by incorporating the local bending effects on the analysis, it is possible to obtain a better estimation of the crack propagation rates, using the VCCT methodology.

There are many published studies that evaluate the effect of bending on the propagation of cracks, demonstrating its importance; however, no studies were found demonstrating the influence exerted by local bending in the propagation phase of short cracks typical of built-up wing panels. The high cost of developing crack propagation tests on panels with representative thicknesses of wings and test rigs required to perform the test could be the reason.

Other methodologies (e.g., energy release method, J-integral, etc.) can be used for this simulation, but VCCT proved to be efficient in obtaining representative results with low computational cost because it uses shell elements, linear materials, and linear solutions.

The study proved, through the correlations presented for different panel configurations, that the prediction of short cracks propagation through the VCCT methodology shall be consider the out-of-plane bending in the calculation of the stress intensity factor (K) and that the superposition principle must be used for the equivalent beta calculation.

7. Contact Author Email Address

mailto: willy.mendonca@embraer.com.br

8. Copyright Statement

References

[1] Corbani S, Martha L F, Castro J T, Carter B, Ingraffea A. Crack front shapes and stress intensity factors in plates under a pure bending loading that induces partial closure of the crack faces. 20th European Conference on Fracture (ECF20), n.3, p. 1279-1284, 2014.

[2] Fawaz S. Application of the virtual crack closure technique to calculate stress intensity factors for through cracks with an oblique elliptical crack front. Delft, 57 p., 1996. Internal Report LR-805 – Delft University of Technology.

[3] Jones D P, Swedlow J L. The influence of crack closure and elasto-plastic flow on the bending of a cracked plate.

International Journal of Fracture, v.11, n.6, p. 897-914, 1975.

[4] Kraft J, Fällgren C, Vormwald M. Calculation of stress intensity factors from shell elements under mixed mode loading. International Journal of Fatigue, v.134, May 2020.

[5] Krueger R. The virtual crack closure technique: history, approach and applications. NASA/CR-2002-211628 ICASE Report No. 2002-10, NASA Langley Research Center Hampton, 2002.

[6] Jokinen J, Kanerva M, Saarela O, Multi-site delamination analysis using virtual crack closure technique for a composite aircraft wing flap. 31st Congress of the International council of the aeronautical sciences (ICAS), 2018.

[7] Palani G S, Iyer N R, Dattaguru B. A generalised technique for fracture analysis of cracked plates under combined tensile, bending and shear loads. Computers and Structures, v.84, p. 2050-2064, 2006.

[8] Roberts R, Erdogan F. The effect of mean stress on fatigue crack propagation in plates under extension and bending. Journal of Basic Engineering, v.89, n.4, p. 885-892, 1967.

[9] Roy M R. Stress intensity factors for ship details. Edinburgh, 141 p., 2009. Thesis – Heriot-Watt University.

[10] Rybicki E F, and Kanninen M F. Finite-element calculation of stress intensity factors by a modified crack closure integral. Engineering Fracture Mechanics, 9(4), pp. 931-938, 1977.

[11] Viz M J, Potyondy D O, Zehnder A T. Computation of membrane and bending stress intensity factors for thin, cracked plates. International Journal of Fracture, n.72, p. 21-38, 1995.

[12]] Williams M L. On the stress distribution at the base of a stationary crack. Journal of Applied Mechanics, 24, pp. 109-114, March, 1957.

[13] Westergaard H M. Bearing pressures and cracks. Journal of Applied Mechanics, pp. A49-A53, June 1939.

[14] Broek D. *The practical use of fracture mechanics*, 1st edition, Springer Dordrecht, 1989.

[15] NASGRO, Fracture mechanics and fatigue crack growth analysis software (version 9.20), reference manual, NASA Johnson Space Center and Southwest Research Institute, 2010.

[16] Han B, Veidt M, Capararo D,George G, Finite element Simulation of crack propagation in military aircraft coatings, 28th International Congress of the aeronautical sciences (ICAS), 2012.

[17] Melo A T A, Nolli B L, Cimini C A, Finite element model development for simultaneous crack propagation in two cooperative lugs, 31st Congress of the International council of the aeronautical sciences (ICAS), 2018.

[18] Shaopu S, Wendong Z, Lei L, Fracture criterion analysis and crack growth property of mixed-mode crack Experiments. 32nd Congress of the International council of the aeronautical sciences (ICAS), 2021.

[19] Zaplana L, Rivero I, Fogeda B G, Escalonilla J G, Fatigue and crack propagation life improvement quantification for cold-worked holes outside nominal conditions. 31st Congress of the International council of the aeronautical sciences (ICAS), 2018.